**Klaus Scheffler**
**Stefan Lehnhardt**

# Principles and applications of balanced SSFP techniques

K. Scheffler (✉)
Department of Medical Radiology,
MR-Physics,
University Hospital,
Petersgraben 4, 4031 Basel, Switzerland
e-mail: klaus.scheffler@unibas.ch
Tel.: +41-61-2655557
Fax: +41-61-2655351

S. Lehnhardt
Department of Diagnostic Radiology,
University Hospital of Freiburg,
Hugstetterstrasse 55, 79106 Freiburg,
Germany

**Abstract** During the past 5 years balanced steady-state free precession (SSFP) has become increasingly important for diagnostic and functional imaging. Balanced SSFP is characterized by two unique features: it offers a very high signal-to noise ratio and a T2/T1-weighted image contrast. This article focuses on the physical principles, on the signal formation, and on the resulting properties of balanced SSFP. Mechanisms for contrast modification, recent clinical application, and potential extensions of this technique are discussed.

## Introduction

Although formally described in 1958 by Carr [2] balanced steady-state free precession (SSFP) has only become feasible (and popular) during the past 3–5 years. At the same time several new acronyms for balanced SSFP have been created such as TrueFISP, balanced FFE, and FIESTA. In several publications and conference abstracts balanced SSFP is just called SSFP to emphasize that the magnetization is acquired during the steady state. This is very confusing and wrong, since all rapid gradient-echo sequences are SSFP sequences, even the radio-frequency-spoiled fast low-angle shot (FLASH; SPGR, T1-FFE) sequence. Different steady states are established for different gradient switching patterns. The most important types of SSFP sequences are the FLASH (GRASS, FAST, FFE), the CE-FAST (PSIF, T2-FFE), and balanced SSFP sequence. This article gives an overview of the basic physical principles of balanced SSFP, a detailed description of contrast- and signal-to-noise mechanisms, and potential image arti-

facts. Different possibilities to modify the generic contrast of balanced SSFP are described in the second part, followed by a short overview of current clinical applications, and examples of possible extensions.

## Physical principles of balanced SSFP

Each type of gradient-echo (GE) sequence consists of a train of excitation pulses that are separated by a constant time interval (TR). The acquisition and the spatial Fourier encoding of the gradient echo is performed between consecutive excitation pulses by means of switched gradient pulses along read, phase, and slice direction. The effect of excitation and gradient pulses on a single magnetization vector can be described by the Bloch equation [1]. As depicted in Fig. 1, an excitation pulse corresponds to a rotation of the magnetization vector by a certain angle $\alpha$ (the flip angle), whereas dephasing (induced by gradient pulses or other field inhomogeneities) is equivalent to a rotation around the z-axis. The amount of
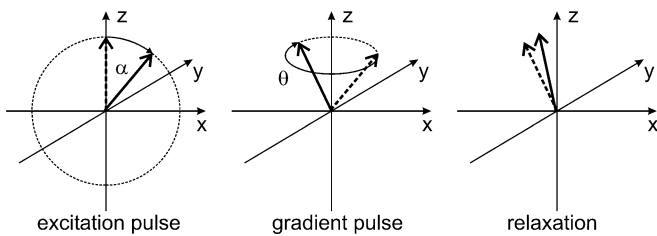
Fig. 1 Evolution of the magnetization within one TR cycle. The excitation pulse rotates the magnetization by an angle of α from the initial z-position towards the transverse plane. The phase of the excitation pulse is along the y-axis. Dephasing due to switched gradients or field inhomogeneities corresponds to a certain rotation around the z-axis. Relaxation during TR leads to a decrease of the transverse component (T2) and an increase of the z-component (T1)
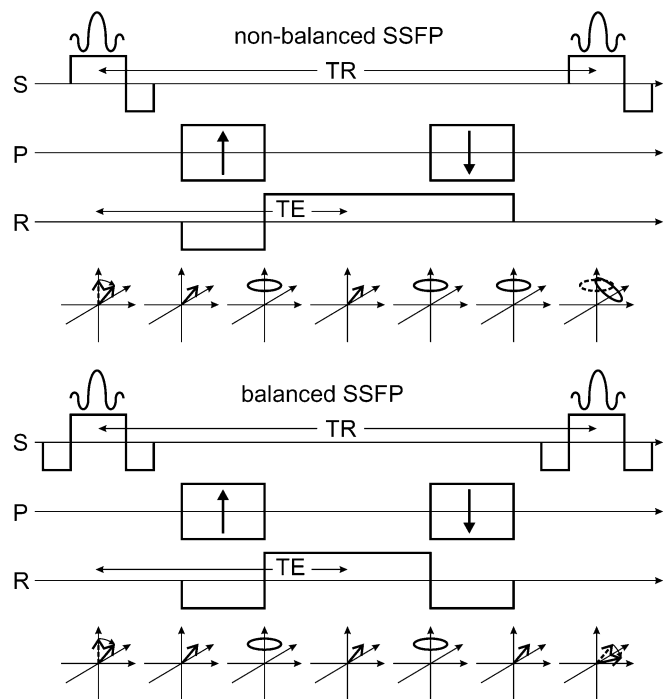


Fig. 2 Evolution of the magnetization within one TR period for a nb-SSFP (refocused FLASH) and a b-SSFP sequence. For nb-SSFP, the readout gradient is not balanced resulting in dephased magnetization after one TR period. For b-SSFP, all three gradient axes are refocused or balanced leading to a single magnetization vector at the end of TR

dephasing θ within TR depends on the spatial position and on the gradient strength and duration. In addition to these rotations, T1 and T2 relaxation occurs during TR. T1 relaxation results in a small increase of the longitudinal component of the magnetization vector, and T2 relaxation gives a shortening of the transverse part by a factor of exp(-TR/T2). After one TR, the next excitation pulse acts on the modified magnetization, and the process of rotation and relaxation is repeated again and again. It can be shown that under certain conditions (constant α, θ, and TR) a steady state of the magnetization will be established after several TR periods (~5T1/TR). This situation is called steady-state free precession (SSFP) and was formally first described by Carr [2]. All types of currently used, fast GE sequences are SSFP techniques. The difference between the various types of GE sequences, such as FLASH, FAST, GRASS, FFE, CE-FAST, and PSIF, is a different gradient switching patter applied between consecutive excitation pulses. Different gradient time courses produce different (spatially dependent) dephasings θ within TR, which finally results in different types of steady states, and more importantly, in different image contrasts.

Balanced SSFP is a special type of SSFP sequence where the gradient-induced dephasing within TR is exactly zero [3]. In other words, within TR each applied gradient pulse is compensated by a gradient pulse with opposite polarity. This makes the pictorial description of the evolving magnetization from excitation pulse to excitation pulse very simple and concise. The overall magnetization consists of a single magnetization vector that is not spatially dephased, as for non-balanced SSFP sequences.

Evolution of the magnetization within TR

In a first step we analyzed the motion of the magnetization within one TR period for the balanced SSFP

(b-SSFP) and non-balanced SSFP (nb-SSFP, such as FLASH or GRASS) sequence (Fig. 2). The first excitation pulse turns the equilibrium magnetization by an angle of α into the transverse plane. The gradient applied in z-direction during the excitation pulse is used for slice selection (S). Conventional slice selective excitation pulses (sinc or Gaussian shaped) applied together with a slice selection gradient produce a linear dephasing of the magnetization along slice select direction, and a second slice selection gradient with opposite polarity has to be applied to refocus the magnetization; therefore, for both b-SSFP and nb-SSFP sequences the resulting magnetization after the slice selection gradient is a single, rephased magnetization vector tilted by an angle of α away from the z-axis. The following gradients are used for frequency (read gradient) and phase encoding (P and R axis).

For simplicity we assume that we are just encoding the center line of k-space, which means that the phase-encoding gradient is zero. Then, the negative lobe of the read gradient induces a dephasing of the previously aligned magnetization. The dephasing is compensated by the positive gradient lobe, and neglecting other field inhomogeneities, the magnetization will be rephased at TE to form again a single magnetization vector (the gradient echo). Until this point (TE) b-SSFP and nb-SSFP are still equivalent. After TE, the magnetization will be de-

phased again by the read gradient. For b-SSFP this dephasing is compensated with a negative read gradient lobe, resulting again in a fully refocused, single magnetization vector. The read gradient is not balanced for nb-SSFP, and the final magnetization is evenly distributed on a disk in the transversal plane. This is the main difference between b-SSFP and nb-SSFP: the net transverse magnetization after one TR is zero for nb-SSFP; for b-SSFP the magnetization at the beginning of the TR interval (just after the excitation pulse) and at the end of the TR interval (just before the next excitation pulse) is nearly identical, except for some T1 and T2 relaxation effects.

The next excitation pulse thus acts on a single magnetization vector. For nb-SSFP the second excitation pulse partially turns the disk of dephased magnetization into the transverse plane, and the dephasing within TR creates an increasingly complicated pattern of dephased magnetization. These increasingly higher states of dephased magnetization form a very interesting 3D pattern of dephased magnetization. The analysis and description of these states is actually much more complicated than the fully refocused magnetization of the b-SSFP sequence. A pictorial description of rapid SSFP imaging is given by Scheffler [4].

### The b-SSFP excitation pulse train

For reasons explained later, the b-SSFP excitation train consists of an initial $\alpha/2$ preparation pulse followed by a train of alternating $\pm\alpha$ excitation pulses [5]. The $\pm\alpha$ pulses are separated by TR, whereas the time interval between the $\alpha/2$ preparation pulse and the first $-\alpha$ pulse is TR/2. Since we know that the switched gradient pulses between consecutive excitation pulses have no influence on the magnetization, it is very easy to analyze the motion of the magnetization during such an excitation pulse train. If we further neglect relaxation effects, the motion of the magnetization becomes a very simple oscillation around the z-axis, as shown in Fig. 3a. The initial $\alpha/2$ pulse brings the magnetization immediately into its steady state position, and subsequent alternating $\pm\alpha$ pulses produce the oscillation around the z-axis. The amplitude of the echo signal is $M_0\sin(\alpha/2)$ which corresponds to the transverse part of the magnetization vector.

A very similar behavior is observed if relaxation is included. As depicted in Fig. 3b (left), the magnetization vector still oscillates around the z-axis, but relaxation produces a certain damping of the magnetization. All magnetization vectors are aligned on a $\alpha/2$ cone and the amplitude of their transverse part converges toward the steady sate. The resulting smooth decay of the transverse magnetization $M_T$ is shown in Fig. 3b (right). From these figures it is also clear that is very beneficial to start the excitation pulse train with an $\alpha/2$ preparation pulse. This
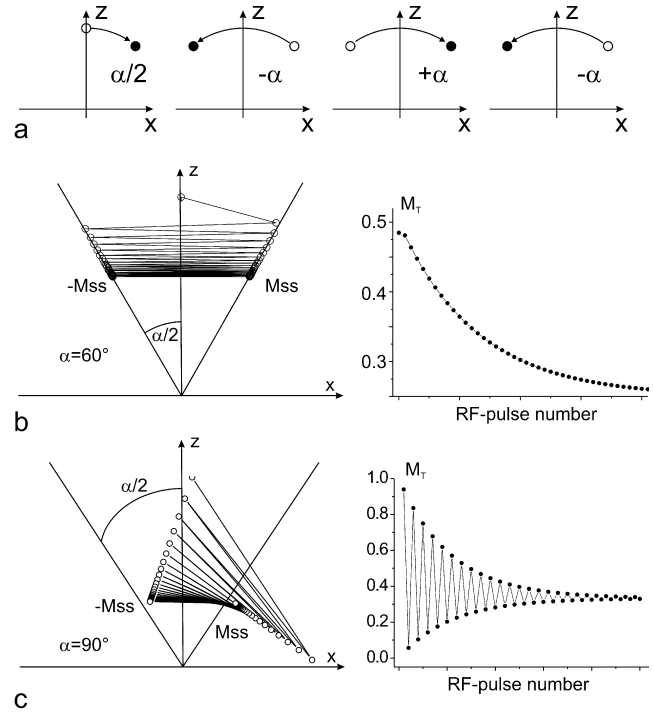


**Fig. 3 a** Starting with an initial $\alpha/2$ preparation pulse the magnetization describes a simple oscillation around the z-axis by means of alternating $\pm\alpha$ excitation pulses. **b** If relaxation is included, a smooth damping of the oscillation can be observed towards a certain, oscillating steady state. **c** The same steady state will be reached without $\alpha/2$ preparation pulse, but the resulting initial fluctuations cannot be used for image acquisition

preparation pulse aligns the magnetization onto the $\alpha/2$ cone resulting in a smooth approach towards the steady sate. The same steady state will also be reached without the $\alpha/2$ preparation pulse, as shown in Fig. 3c; however, the intense initial signal fluctuations would produce severe image artifacts and can thus not be used for signal acquisition.

### Sensitivity of b-SSFP to off-resonance effects

Up to now, we have assumed that we have a perfect shim across the entire field of view (FOV), or equivalently, the absence of any dephasing of the magnetization between excitation pulses. In typical applications the achievable field homogeneity is approximately 50 Hz for the brain, and 100–200 Hz for the abdomen at 1.5 T. A frequency offset $\nu$ (frequency difference between radio-frequency synthesizer of scanner and local precession frequency of the magnetization) results in a dephasing of $\theta=2\pi\nu TR$ within TR. This is, for example, 108° for TR=3 ms and $\nu$=100 Hz. It is obvious that this additional dephasing leads to a modification of the resulting steady state, and hence to a certain deviation from the ideal os-
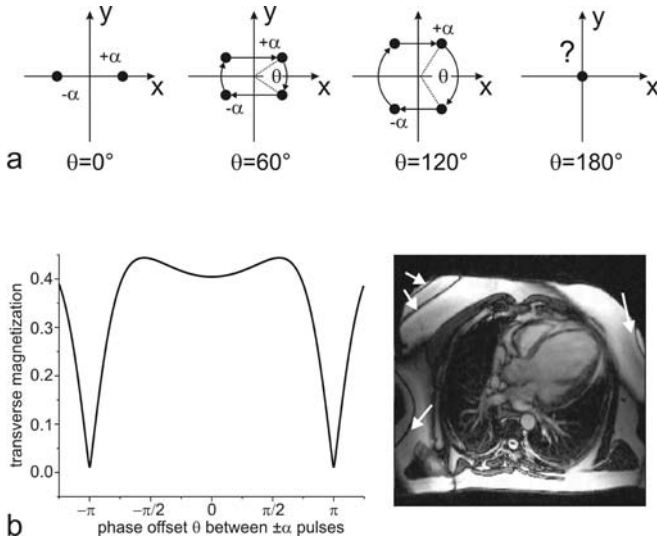
**Fig. 4 a** The motion of magnetization (*filled circles* correspond to the tip of the magnetization, projected onto the x–y plane) during one TR for different dephasings θ. For increasingly higher dephasings θ the trajectory shows an increasingly higher deviation from the simple oscillation around z. The steady state breaks down for θ=180°. **b** The steady-state signal amplitude of b-SSFP as a function of the dephasing between TR. This profile is characterized by a brought plateu interrupted by sharp signal drops. The b-SSFP thus provides high signal amplitudes within some range of different off-resonance frequencies but shows a strong signal loss if dephasing is near multiples of 2π. This leads to the well-known banding artefacts as shown right (*arrows*)

cillation around the z-axis (Fig. 3b). Fortunately, these deviations are relatively small (for small off-resonance frequencies). Figure 4a depicts the positions of the steady-state magnetization for increasingly higher dephasing θ within TR (or higher off-resonance frequencies). Due to the off-resonance frequency, the magnetization performs a rotation around the z-axis by an angle of θ=2πνTR between alternation excitation pluses (top view, projection onto the transverse plane).

Interestingly, this dephasing starts at an angle of θ/2 away from the x-axis and ends at the position –θ/2. In other words, at the echo time TE=TR/2 the magnetization vector is exactly aligned along the x-axis, independent of the total dephasing θ. This refocusing mechanism is very similar to the spin-echo formation. The refocusing mechanism breaks down above some certain point of dephasing, leading to a nearly complete collapse of the steady-state signal. This threshold lies somewhat below θ=π and can be visualized by the amplitude-frequency profile of b-SSFP (Fig. 4b).

This profile gives the steady-state amplitude of b-SSFP as a function of some field inhomogeneity-induced dephasing θ within TR [2]. It is a 2π-periodic profile that shows very sharp and significant signal drops at ±π. This specific signal profile as a very important consequence for b-SSFP imaging: the signal amplitude depends on the

local shim! For example, if we assume a variation of ±200 Hz across the FOV and a TR of 3 ms, we will have different dephasings between −216° and +216° at different spatial locations. This leads to the well-known banding artifacts, characterized by strong signal drops at regions where θ=±π or ν=±167 Hz for TR=3 ms. An example is shown in Fig. 4b (right). For banding-free imaging the allowed range of different off-resonance frequencies has thus to be confined to approximately $\pm \frac{1}{2TR}$.

From these calculations it is immediately clear that b-SSFP benefits from very short TR that allows covering a brought range of off-resonance frequencies. In other words, a short TR makes b-SSFP less sensitive to field inhomogeneities.

Contrast and signal-to-noise of b-SSFP

Besides potential image artifacts, the most important feature of an imaging sequence is its contrast. While the classical SE sequence either shows a T1- or a T2-weighted contrast (or proton-density-weighted), rapid GE sequences, including b-SSFP, exhibit a relatively complicated contrast that is composed (it is not just a product) of T1 and T2 contributions. The steady-state signal intensity of b-SSFP has already been shown in Fig. 4b for different off-resonance frequencies. On-resonance the resulting signal intensity is a function of T1, T2, TR, and flip angle α, and is given by

$$M_{SS} = M_0 \frac{\sqrt{E_2(1-E_1)}\sin\alpha}{1-(E_1-E_2)\cos\alpha - E_1 E_2}, \tag{1}$$

with $E_{1,2} = e^{-TR/T1,2}$, and $M_0$ is the proton density [6, 7]. This equation can be simplified under the assumption that $TR \ll T_1, T_2$ (which is the case for most biological tissue at 1.5 T and a TR of 3–5 ms) [8]:

$$M_{SS} = M_0 \frac{\sin\alpha}{1+\cos\alpha+(1-\cos\alpha)(T1/T2)}. \tag{2}$$

Figure 5 shows the signal intensity of b-SSFP for different ratios of T1 and T2 as a function of the flip angle α. The optimal flip angle depends on T1 and T2 and is given by

$$\cos(\alpha) = \frac{T_1/T_2 - 1}{T_1/T_2 + 1}, \tag{3}$$

which results in a signal amplitude of [8]:

$$M_{SS} = \frac{1}{2} M_0 \sqrt{T_2/T_1} \tag{4}$$

If T1 and T2 are similar (i.e. for CSF or fat) the optimal flip angle is around α=70–90°, and the maximum possible signal approaches 50% of $M_0$! This is a very remarkable feature of b-SSFP, and there exists no other type of sequence that is able to continuously acquire 50% of the
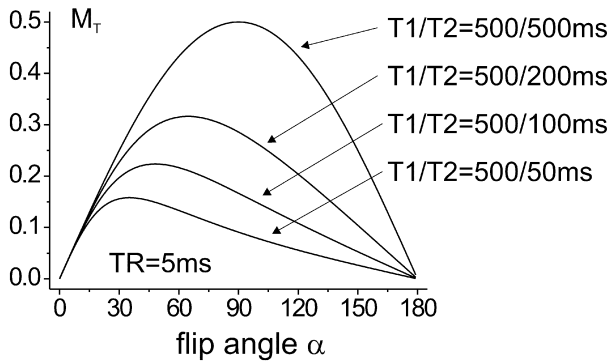
**Fig. 5** Steady state signal intensity as a function of the applied flip angle. For similar T1 and T2 the signal approaches 50% of $M_0$ for a flip angle of 90°
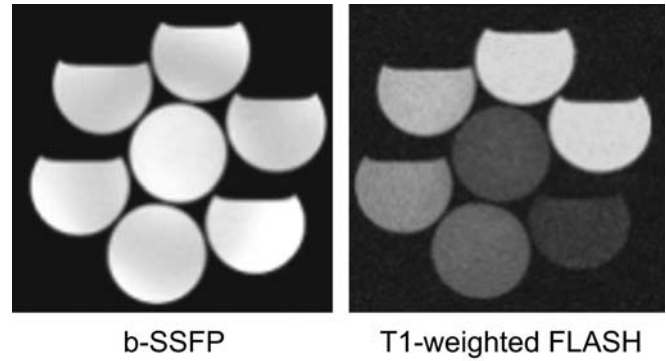


**Fig. 6** The b-SSFP and nb-SSFP (T1-weighted FLASH) image of bottles filled with water and different concentrations of a conventional gadolinium-based contrast agent. Since reduction of T1 and T2 is similar the ratio T2/T1 is nearly independent of the concentration of the contrast agent leading to comparable signal intensities for b-SSFP. A clear T1 contrast can be observed for T1-weighted FLASH

total available spin polarization $M_0$! Based on its totally coherent steady-state magnetization, b-SSFP thus offers the highest possible signal-to-noise ratio (SNR) per unit time of all known sequences.

However, the contrast of b-SSFP is given by the ratio of T2 and T1, which is certainly not optimal for diagnostic purposes. A typical feature of the b-SSFP contrast is the very high signal intensity of liquids and fat (both have completely different T1 and T2 values, but a similar ratio of T2 and T1; see Fig. 4b), which cannot be seen on purely T1- or T2-weighted sequences. A further example is shown in Fig. 6. The bottles are filled with water and different concentrations of a gadolinium-based contrast agent, resulting in T1 values between 100 and 1500 ms. For b-SSFP the signal intensities of different bottles are nearly identical since the contrast agent reduces both T2 and T1 (the relaxivities R2 and R1 of the contrast agent are similar). A clearly T1-weighted contrast can be observed for the radio-frequency-spoiled FLASH sequence.

For the sake of completeness it is noted that the echo amplitude $M_{SS}$ of b-SSFP is not additionally weighted by a factor of exp(-TE/T2*) as for the FLASH sequence. B-SSFP does not show the conventional T2* sensitivity as other nb-SSFP sequences. This can be explained by the fact that, within a certain range, field inhomogeneity-induced dephasing will be nearly completely refocused at TE=TR/2 leading to the formation of a spin echo rather than a gradient echo [9]. As already included in Eq. (1), the steady state signal $M_{SS}$ of b-SSFP is thus additionally weighted by exp(-TE/T2) which is equal to

$$\sqrt{E_2} \text{ for TE} = TR/2 \qquad (5)$$

## Further contrast mechanisms

So far we have focused on the steady state contrast of b-SSFP. The signal intensity during the transition to the steady state, however, shows a remarkably different behaviour. The duration of the transient phase is of the order of 50–500 excitation pulses, as shown in Fig. 3. It can be shown that the decay rate towards the steady state is a weighted average between a pure T1 and a pure T2 decay. For very small flip angles ($\alpha$) the decay is mainly controlled by T1. High flip angles produce a faster decay towards the steady state. For $\alpha$=180°, the signal decays exactly with T2 towards zero ($M_{SS}$=0 for $\alpha$=180°; see Eq. (1)). This case is actually very similar to a multi-spin-echo sequence such as rapid acquisition with relaxation enhancement (RARE): both sequence types start with a 90° excitation pulse followed after TR/2 by 180° refocusing pulses separated by TR (echo spacing for RARE).

Due to the relatively long duration of the transient phase of b-SSFP, the contrast of 2D images compared with 3D images is quite different, as shown in Fig. 7. The 2D image exhibits a mixed contrast between proton density and $\sqrt{T_2/T_1}$. The 3D image shows the pure steady-state contrast characterized by a loss of contrast between grey and white matter, and an increased signal of fat and cerebrospinal fluid.

Inflow or motion effects can further modify the contrast of b-SSFP, as shown for two examples in Fig. 8. An especially high contrast between the transient signal of inflowing blood and the steady-state signal of muscle (which is low due to a low T2/T1 ratio) can be observed, which makes b-SSFP very useful for cardiac imaging. No inflow enhancement can be created in 3D applications as shown right (with fat saturation), resulting in a similar steady-state contrast of blood and other tissues.
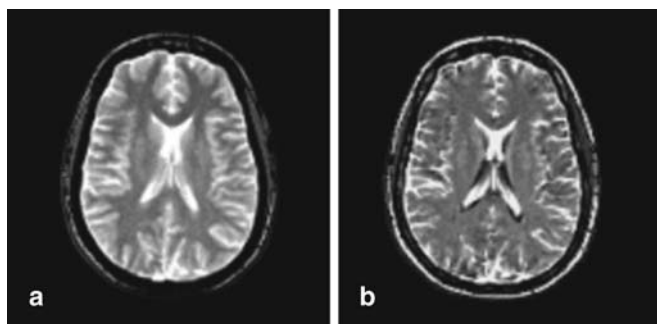
**Fig. 7** A 2D b-SSFP acquisition shows **a** transient contrast compared with **b** the T2/T1-weighted steady-state contrast of 3D b-SSFP
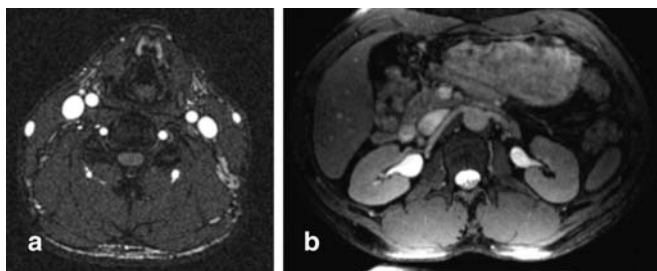


**Fig. 8** 2D b-SSFP shows **a** inflow enhancement (the time-of-flight effect) which cannot be observed in **b** 3D applications (right, with fat saturation)

Implementation of b-SSFP

Balanced SSFP requires short TR in the range of 3–6 ms to minimize banding artefacts. This is the main reason why b-SSFP, although proposed in 1986 by Oppelt et al. [3], has only become feasible (and popular) during the past 3–5 years. With the design of very fast gradient amplifiers it was possible to reduce the time to switch all relevant gradients needed for echo encoding to a few milliseconds. During the past years each manufacturer invented its own acronym for b-SSFP, for example, TrueFISP (Siemens, originally call FISP by Oppelt et al. [3]), balanced FFE (Philips), or FIESTA (GE). A slow version of b-SSFP, called CISS (constructive interference in steady state), with TR of approximately 15–20 ms was introduced approximately 10 years ago. The CISS consists of two consecutive 3D b-SSFP runs. The first b-SSFP part uses alternating $\pm\alpha$ excitation pulses, and the second b-SSFP run is performed with constant $\alpha$ pulses. As a result, two image sets are acquired that show mutually shifted banding artefacts. A maximum intensity projection (or a more sophisticated algorithm) between these two data sets gives the banding-free CISS image.

The minimum possible TR for b-SSFP is comparable to the TR of rapid GE sequences that are used for CE

MRA; However, b-SSFP requires relatively high flip angles between 50–80° to generate the highest possible signal. This can easily exceed the SAR limits, especially in ultra-high field applications beyond 1.5 T. A possibility to reduce SAR is the use of optimized slice excitation pulses, or to apply varying flip angles during the excitation pulse train [10, 16].

## Modification of the generic b-SSFP contrast: magnetization preparation

The modification and optimization of the contrast of an imaging sequence with certain magnetization preparation techniques, such as inversion or fat saturation pulses, is a common method that has been widely applied in combination with FLASH or RARE sequences [11, 12]. Typical examples are the FLAIR or STIR sequence (combination of inversion pulse with RARE-based acquisition block), or the MPRAGE sequence (inversion pulse and FLASH sequence). In the ideal case, the contrast of magnetization-prepared sequences is exclusively generated by the preparation scheme, and the subsequent signal or image acquisition block is just used to detect the prepared magnetization; therefore, the acquisition block should not introduce an additional contrast to the already prepared magnetization, and, in terms of SNR, it should be as effective as possible. B-SSFP is thus ideally suited to read-out prepared magnetization.

Several approaches have already been proposed to modify the non-specific T2/T1-weigthed contrast of b-SSFP. The single-shot methods are comparable to the existing methods based on FLASH or RARE. The steady-state magnetization preparation techniques represent conceptually new approaches that rely on the special magnetization trajectory of b-SSFP.

Single-shot magnetization preparation

The basic scheme of this preparation technique is shown in Fig. 9 [5, 13]. In principle, any known type of magnetization preparation can be used to modify the b-SSFP signal. The use of inversion or saturation pulses has been proposed, for example, to enhance the contrast between grey and white matter, or to introduce T1-weighting. Inversion-prepared b-SSFP can also be used for rapid T1 quantification as shown in Fig. 10. A further application to assess blood perfusion in the kidney based on arterial spin labelling is shown in Fig. 10. Labelling was achieved by selective inversion of the inflowing aortic blood [14]. Further possibilities to combine magnetization preparation with b-SSFP may include T2*, T2, or diffusion preparation, or a combination of them.

As for other magnetization-preparation techniques it is important to notice that the prepared contrast is par-
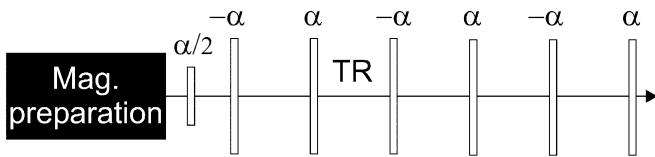
**Fig. 9** Basic principle of single-shot magnetization-prepared b-SSFP. After preparation, b-SSFP is started with an α/2 preparation pulse



**Fig. 11** Principle of contrast modification during the steady state of b-SSFP. The steady-state magnetization is stored in z-direction before magnetization praparation, and is recalled after preparation
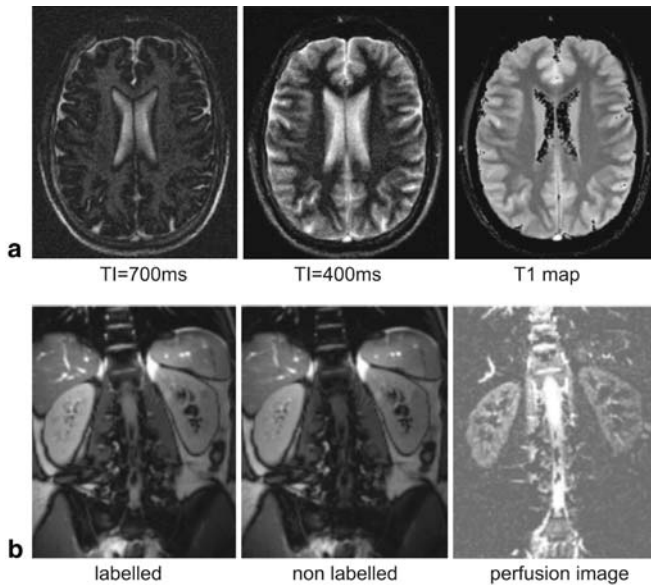


**Fig. 10 a** Series of b-SSFP images acquired after different inversion times after a slice-selective inversion pulse. This series can be used to derive quantitative T1 maps, as shown right. **b** Selective inversion pulse along the descending aorta was applied as a magnetic label for inflowing blood (arterial spin labelling). Subtraction of a non-labelled with a labelled acquisition gives the perfusion image of the kidneys (*right*)

tially modified by the b-SSFP contrast; however, if the time between preparation and encoding of the central k-space line is short (i.e. in segmented or centric reordered acquisitions) these deviations are relatively small. A more severe problem are initial signal fluctuations that may occur during the first 10–30 repetitions of the b-SSFP excitation train. As described previously, the initial α/2 preparation pulse separated by TR/2 from the first excitation pulse is used to stabilize the transient signal evolution [5]. This preparation scheme, however, partially fails for off-resonance spins leading to similar signal oscillations as shown in Fig. 3c. This is a major problem especially for single-shot techniques, and several approaches have been proposed to stabilize the initial, transient phase. A very robust and simple method is to use linearly increasing flip angles for the first 5–15 excitation pulses [15]. A further possibility is to use the RARE excitation scheme based on a 90° excitation pulse and

180° refocusing pulses, followed by a train of decreasing flip angles towards the final flip angle of 50–70°. This technique is called transition into driven equilibrium (TIDE) and can also be use to modify the contrast of b-SSFP [16]. Further stabilization methods are based on preparation schemes that "catalyze" the required steady-state magnetization [17].

Steady-state magnetization-preparation techniques

In contrast to single-shot techniques steady-state magnetization preparation offers the possibility to incorporate virtually any contrast into a continuously running b-SSFP sequence [18]. This allows for a very efficient contrast modification, since signal acquisition is interrupted only for short periods. In order to maintain the high steady-state signal the periodic interruption of the b-SSFP excitation train with preparation pulses requires a dedicated preparation and non-preparation scheme, as shown in Fig. 11. Before preparation the excitation train is stopped with an α/2 non-preparation pulse that stores the steady-state magnetization in z-direction. After preparation, the stored z-magnetization is used again by means of the α/2 preparation pulse. This technique can be used for rapid, fat-saturated or T2-weighted b-SSFP imaging.

A further possibility to modify the contrast during the steady state is a continuous variation of the flip angles of the excitation pulses. This can be done either with the TIDE technique [16], or by using flip angles that depend on the distance between encoded k-space position and k-space centre [10]. A (non-linear) variation of the phase of the excitation pulses is able to create several-steady states that exhibit different frequency-amplitude response profiles. Selection or combination of different steady states can thus be used to generate spectral-selective images [28, 29].

## Clinical applications of balanced SSFP

From the previously described properties of b-SSFP it can be deduced that b-SSFP has limited application for conventional diagnostic imaging that is based on T1- or T2-weighted techniques; however, b-SSFP is a very fast
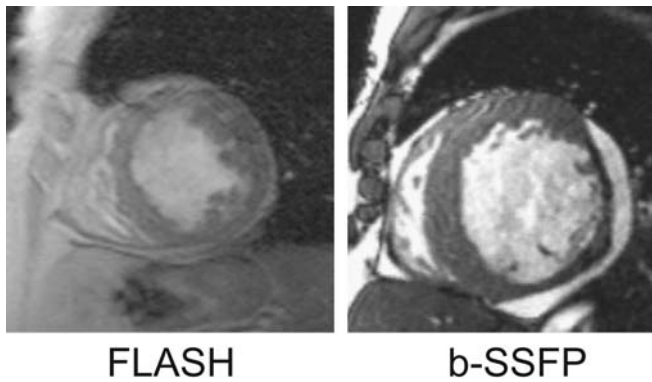
**Fig. 12** Comparison of FLASH and b-SSFP for cardiac imaging

imaging technique that shows a strong contrast between tissues with different rations of T2 and T1, for example, between blood and muscle (or myocardium), between fat and muscle, or between liquid compartments and surrounding tissue. B-SSFP is thus perfectly suited for morphological imaging such as cardiac or vessel imaging. The following examples give a short and non-comprehensive overview of some current clinical applications of b-SSFP.

**Fig. 13a–c** Comparison of different angiography techniques based on b-SSFP. **a** Coronary artery imaging was performed during free breathing using a navigator technique. The b-SSFP was applied for 160 ms during the late diastole preceded by a fat saturation pulse. **b** The TOF acquisition was measured without fat saturation. Background suppression was achieved by repetitive, slice-selective inversion pulses. **c** The use of inversion pulses and contrast agent can be used for contrast enhanced angiography, and offers a significantly higher contrast-to-noise ratio than conventional approaches
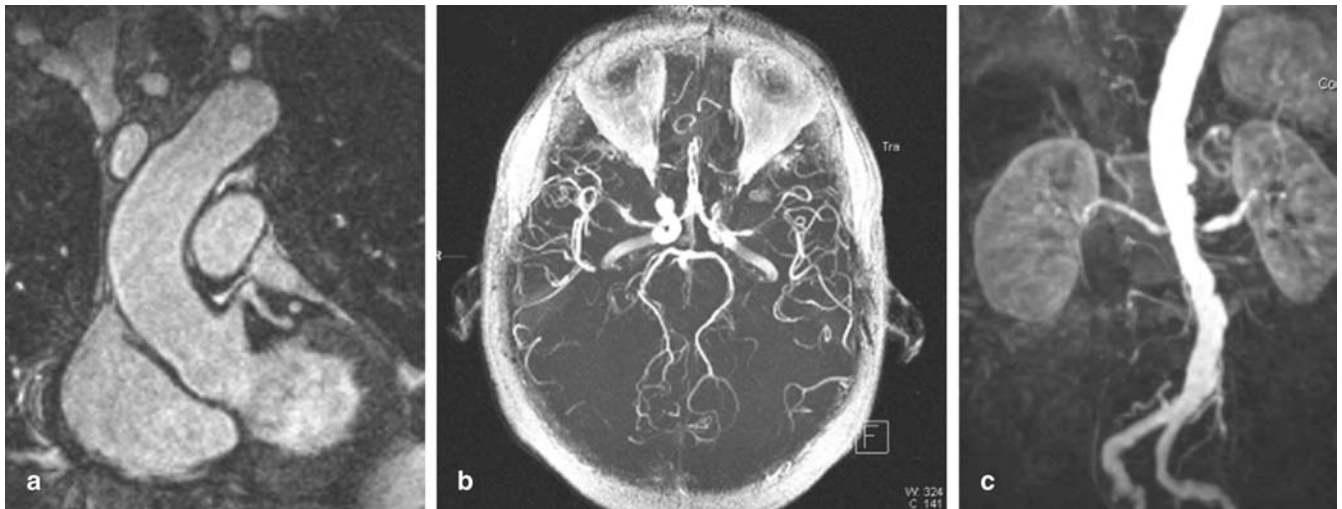
## Cardiac imaging

The motion of the myocardium is conventionally observed with rapid, T1-weighted FLASH sequences [19]. The cine images can then be used to quantify parameters such ejection fraction or ventricular mass. The b-SSFP offers a much higher contrast between muscle and blood than FLASH, which is beneficial for subsequent segmentation algorithms [20, 21]. Figure 12 shows a comparison between FLASH and b-SSFP. The high contrast of b-SSFP is produced both by the different ratio of T2 and T1 of blood and myocardium and by inflow effects. A second advantage of b-SSFP is its high SNR even for very short TR. A FLASH sequence with comparable TR and optimized Ernst flip angle exhibits a much lower SNR and contrast-to-noise ratio (CNR).

## Angiography

The different T2/T1 ratios of blood and surrounding tissue are beneficial for angiografic imaging with b-SSFP; however, depending on the chosen imaging parameters, such as slice thickness and orientation, the observed contrast is actually a mixture of the transient/steady state contrast of b-SSFP and signal-enhancing inflow effects, as depicted in Fig. 8. A major problem of b-SSFP-based angiography is the very intense fat signal that easily exceeds the signal of inflowing blood. An efficient fat saturation is thus mandatory, especially for coronary arteries that are surrounded by fat [22]. Figure 13 shows three different angiography techniques that are based on b-SSFP acquisition. Imaging of the left anterior descending (LAD) coronary artery was performed during free breathing using a navigator technique. The acquisition window was placed within the late diastole, and conventional fat saturation was use prior to b-SSFP acquisition (Fig. 13, left). A different approach was used for time-of-flight (TOF) imaging of the cerebral vessels, shown in
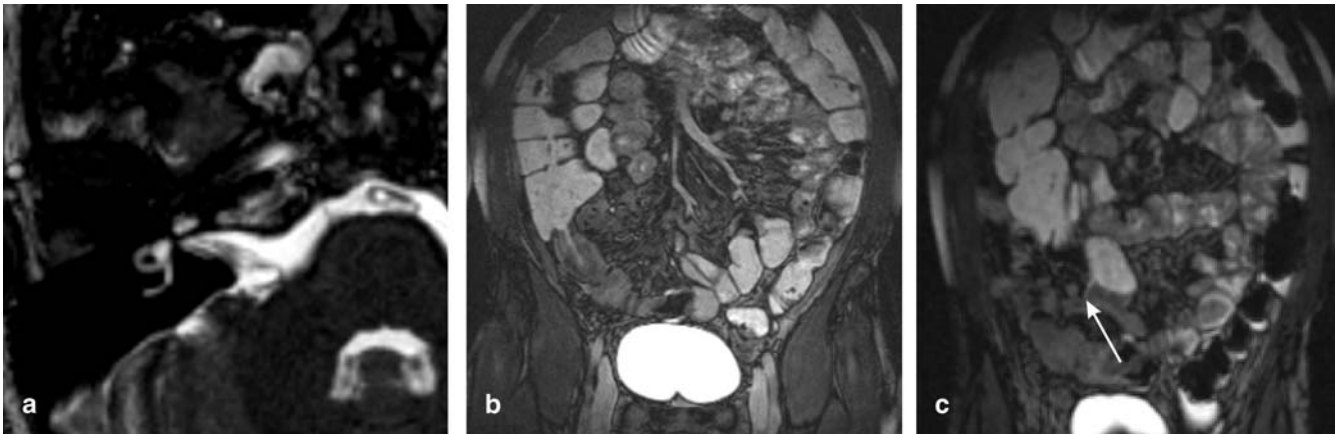
**Fig. 14 a** Conventional and fat-saturated 3D b-SSFP is used to depict and separate tissues or compartments with long T2 relaxation times. **b** Patient with Crohn's disease and multiple stenosis. **c** Patient with Crohn's disease and inflammatory pseudotumor with fistula (*arrow*)

Fig. 13 (middle). The 3D b-SSFP acquisition block was continuously interrupted with a selective inversion pulse for every 1200 ms. As a result, the stationary tissue is nearly completely saturated while inflowing blood shows the full (transient) b-SSFP signal. This new approach offers a significant increase in CNR as compared with conventional 3D TOF techniques [23]; however, no fat saturation was applied for this preliminary application. A further technique that is based on the flow-sensitive phase evolution between excitation pulses was recently proposed for MR angiography [27]. Figure 13 (right) shows an example of contrast enhanced b-SSFP angiography that potentially offers an increase of CNR of up to 100% compared with FLASH-based techniques. The T1 and T2 values of blood during the first pass of a contrast agent are very similar (approximately 50–150 ms) resulting in the highest possible b-SSFP signal of up to 50% of M0. The surrounding tissue was saturated by repetitively applied inversion/saturation pulses, which finally produces an excellent contrast between vessel and background. In this example additional fat saturation was applied immediately before inversion/saturation [24].

## T2-like applications

Balanced-SSFP is certainly not a T2-weighted sequence. Long T2 relaxation times produce high signal intensity, but short T2 times in combination with short T1 times might show the same signal intensity. For the diagnosis of diseases of the abdomen and the liver, the detection of hepatic lesions, the demonstration of the bile duct system and the exact illustration of the vessels, especially in the pre-operative planning, is essential [26]. The mixed contrast of b-SSFP is certainly not optimal for diagnosing hepatic le-

sions. Additionally susceptibility artifacts due to field inhomogeneities and artifacts at tissue interfaces close to the gastrointestinal tract hamper the use of these sequences in the abdomen; therefore, so far there is no evidence for diagnostic use in detection and characterization of hepatic lesions with b-SSFP [30]. This thesis was underlined by a recent study which compared b-SSFP and half-Fourier single-shot turbo spin-echo (HASTE) in the liver. It was found that neither HASTE nor b-SSFP alone are sufficient for detection and characterization of hepatic lesions [31].

A clearer contrast can be achieved if compartments with long T2 are not surrounded by tissues with comparable T2/T1 ratios. Two examples are shown in Fig. 14. The liquid containing inner ear and cranial nerve is clearly separated from the background. This single 3D b-SSFP acquisition shows an identical contrast compared with the CISS technique, and offers a sub-millimetre resolution within an acquisition time of several minutes.

Recently, hydro-MRI in patients with chronic inflammatory disease of the small bowel (Crohn's disease) has been introduced [32]. With the use of T2 HASTE sequences and post-contrast images stenosis, small bowel wall changes and activity of the inflamed wall could be demonstrated. A promising approach of imaging the small bowel could be the use of 3D fat saturated b-SSFP sequences (Fig. 14, middle and right). A sufficient lumen opacification and an increased wall delineation with an improved wall conspicuity could be achieved, which is mainly caused by an improved tissue contrast. Extramural complications can be detected with high diagnostic accuracy. With the use of ultrafast sequences the acquisition time can be reduced, producing fewer motion artefacts. By using 3D sequences during one breath-hold period the possibility of secondary reconstruction, e.g. maximum intensity projection and multiplanar reconstruction, is given [18]. A further (preliminary) field of application is the detection and segmentation of spinal nerve roots where the high signal of CSF offers a good separation to the surrounding tissue [25].

## Conclusion

Balanced SSFP offers the highest SNR per unit time of all other imaging sequences. For an optimized flip angle the resulting contrast is T2/T1-weighted. This type of mixed contrast has limited application for diagnostic imaging, but is beneficial for functional or morphological imaging such as cardiac imaging. Magnetization-preparation techniques can be used to modify the b-SSFP contrast for specific applications. Signal instabilities during the initial phase of the excitation train as well as reduction of radio-frequency power deposition can be achieved with dedicated schemes of varying flip angles of the excitation pulses.

## References

1. Bloch F (1946) Nuclear induction. Phys Rev 70:460–474
2. Carr HY (1958) Steady-state free precession in nuclear magnetic resonance. Phys Rev 112:1693–1701
3. Oppelt A, Graumann R, Barfuss H, Fischer H, Hartl W, Schajor W (1986) FISP: a new fast MRI sequence. Electromedica (Engl Ed) 54:15–18
4. Scheffler K (1999) A pictorial description of steady states in fast magnetic resonance imaging: concept. Magn Res 11:291–304
5. Deimling M, Heid O (1994) Magnetization prepared true FISP imaging. In: Proc Second Annual Meeting of the Society of Magnetic Resonance, San Francisco, p 495
6. Freeman R, Hill HDW (1971) Phase and intensity anomalies in Fourier transform NMR. J Magn Reson 4:366–383
7. Zur Y, Stokar S, Bendel P (1988) An analysis of fast imaging sequences with steady-state transverse magnetization refocusing. Magn Reson Med 6:17–193
8. Haacke EM, Brown RW, Thompson MR, Venkatesan R (1999) In: Magnetic resonance imaging: physical principles and sequence design. Mosby, St. Louis, chap. 18
9. Scheffler K. Hennig J (2003) Is TrueFISP a spin-echo or gradient-echo sequence? Magn Reson Med 49:395–397
10. Schaeffter T, Weiss S, Börnert P (2002) A SAR-reduced steady-state free precessing (SSFP) acquisition. Proc ISMRM, Honolulu, p 2351
11. Haase A (1990) Snapshot FLASH MRI: applications to T1, T2, and chemical-shift imaging. Magn Reson Med 13:77–89
12. Norris D, Börnert P, Reese T, Leibfritz D (1992) On the application of ultrafast RARE experiments. Magn Reson Med 27:142–164
13. Scheffler K, Hennig J (2001) T1 quantification with inversion recovery TrueFISP. Magn Reson Med 45:720–723
14. Scheffler K, Thiel T, Thesen S (2002) Assessment of perfusion with arterial spin labeling and TrueFISP. Proc ISMRM, Honolulu, p 628
15. Nishimura DG, Vasanawala SS (2000) Analysis and reduction of the transient response in SSFP imaging. Proc 8th Annual Meeting ISMRM, p 301
16. Hennig J, Speck O, Scheffler K (2002) Optimization of the signal behavior in the transition to driven equilibrium in steady-state free precession sequences. Magn Reson Med 48:801–809
17. Hargreaves BA, Vasanawala SS, Pauly JM, Nishimura DG (2001) Characterization and reduction of the transient response in steady-state MR imaging. Magn Reson Med 46:149–158
18. Scheffler K, Heid O, Hennig J (2001) Magnetization preparation during the steady state: 3D fat saturated TrueFISP. Magn Reson Med 45:1075–1080
19. Wagner S, Buser P, Auffermann W, Holt WW, Wolfe CL, Higgins CB (1989) Cine magnetic resonance imaging: tomographic analysis of left ventricular function. Cardiol Clin 7:651–659
20. Barkhausen J, Ruehm SG, Goyen M, Buck T, Laub G, Debatin JF (2001) MR evaluation of ventricular function: true fast imaging with steady-state precession versus fast low-angle shot cine MR imaging: feasibility study. Radiology 219:264–269
21. Jung BA, Hennig J, Scheffler K (2002) Single-breathhold 3D-trueFISP cine cardiac imaging. Magn Reson Med 48:921–925
22. Deshpande VS, Shea SM, Laub G, Simonetti OP, Finn JP, Li D (2001) 3D magnetization-prepared TrueFISP: a new technique for imaging coronary arteries. Magn Reson Med 46:494–502
23. Leupold J, Hennig J, Scheffler K (2002) 3D time-of-flight MRI using inversion recovery TrueFISP. Proc ISMRM, Honolulu, p 138
24. Scheffler K, Winterer JT, Langer M, Hennig J (2002) Contrast-enhanced angiography using T1-weighted TrueFISP. Proc ISMRM, Honolulu, p 139
25. Amartur SC, Wielopolski PA, Kormos DW, Modic MT, Clampitt M (1991) Tissue segmentation for three-dimensional display of human spines. Med Phys 18:305–308
26. Lienemann A, Anthuber C, Baron A, Kohz P, Reiser M (1997) Dynamic MR colpocystorectography assessing pelvic-floor descent. Eur Radiol 7:1309–1317
27. Overall WR, Conolly SM, Nishimura DG, Hu BS (2002) Oscillating dual-equilibrium steady-state angiography. Magn Reson Med 47:513–522
28. Vasanawala SS, Pauly JM, Nishimura DG (2000) Linear combination steady-state free precession MRI. Magn Reson Med 43:82–90
29. Hardy CJ, Dixon WT (2002) Steady-state free precession imaging with inherent fat suppression. Proc ISMRM, Honolulu, p 473
30. Petsch R, Helmberger T, Reiser M (1999) New techniques and pulse sequences in MRI of the liver. Radiologe 39:662–670
31. Herborn CU, Vogt F, Lauenstein TC, Goyen M, Debatin JF, Ruehm SG (2003) MRI of the liver: Can TrueFISP replace HASTE? J Magn Reson Med 17:190–196
32. Rieber A, Aschoff A, Brambs HJ (2000) MRI in the diagnosis of small bowel disease: use of positive and negative oral contrast media in combination with enteroclysis. Eur Radiol 10:1377–1382